Characterizing the Effects of Ionospheric Divergence and Decorrelation on LAAS

Boris Pervan[*], Sam Pullen[†], John Andreacchi[*], and Per Enge[†]

[*]*Illinois Institute of Technology*
[†]*Stanford University*

BIOGRAPHIES

Boris Pervan received a B.S. from the University of Notre Dame (1986), M.S from the California Institute of Technology (1987), and Ph.D. from Stanford University (1996), all in Aerospace Engineering. From 1987 to 1990, he was a Systems Engineer at Hughes Space and Communications Group. Dr. Pervan was a Research Associate at Stanford from 1996 to 1998, serving as project leader for GPS Local Area Augmentation System (LAAS) research and development. He was the 1996 recipient of the RTCA William E. Jackson Award and the 1999 M. Barry Carlton Award from the IEEE Aerospace and Electronic Systems Society. Currently, Dr. Pervan is Assistant Professor of Mechanical and Aerospace Engineering at the Illinois Institute of Technology in Chicago.

Sam Pullen received two S.B. degrees (in Aeronautics/ Astronautics and History) from the Massachusetts Institute of Technology (1989) and received M.S. (1990) and Ph.D. (1996) degrees from Stanford University in Aerospace Engineering. Since graduating, Dr. Pullen has served as Research Associate and as Technical Manager at Stanford, where he has supported GPS Local Area Augmentation System (LAAS) and Wide Area Augmentation System (WAAS) research and development and now serves as the project leader for LAAS. His work in these fields and his support of the Johns Hopkins University Applied Physics Laboratory (JHU/APL) GPS Risk Assessment earned him the ION Early Achievement Award in 1999.

John Andreacchi received a B.S. in Mechanical Engineering from Northern Illinois University (1996) and M.S. in Mechanical and Aerospace Engineering from Illinois Institute of Technology (2000). Mr. Andreacchi was a design/process engineer in the automotive industry from 1996 to 1999. From 1999 to 2000 he was a Research Assistant in the Navigation and Guidance Laboratory where he studied the effect of Ionospheric Divergence on Differential GPS implementations of code-carrier smoothing filters.

ABSTRACT

In the Local Area Augmentation System (LAAS), as well as other local area DGPS systems which use single-frequency (L1) measurements only, differential ranging error due to the ionosphere is the result of two effects: the temporal divergence of the code and carrier and spatial decorrelation of delay. The effect of divergence is most significant when ground and air filter implementations are different; but even when filter implementations are identical, transient differential error can exist due to the different filter start times. The effect of spatial decorrelation is caused by variations in the delay between the ionospheric pierce points for the aircraft and the ground receiver. The effective separation between ground and aircraft antennas that defines pierce point separation is larger than the physical separation of the two antennas by an amount proportional to the filter time constant and the horizontal velocity of the aircraft. In this work, both ionospheric spatial decorrelation and divergence are analyzed with the goal of defining conditions for safe interoperability of ground and airborne systems.

1.0 INTRODUCTION

In the Local Area Augmentation System (LAAS), L1 pseudorange and carrier phase measurements are brought together by means of a smoothing filter. The filter exploits the accuracy of the pseudorange (raw code phase) and the higher precision of the carrier phase to mitigate multipath and other receiver-associated noise. Among several errors embedded in the smoothed pseudorange, the one of interest in this paper is the filtered output of the ionosphere-induced group delay and phase advance. The carrier phase advance and pseudorange code delay are equal and opposite. Thus over time, the effect is realized as a divergence between the code and carrier measurement error. When such a diverging error is filtered, there will exist, in general, a tracking error in the output of the smoothing filter relative to the raw code pseudorange. The nature and magnitude of the tracking error is a function of the filter used and the time history of ionospheric divergence [1]. For example, the LAAS Ground Facility (LGF), which will use single-frequency measurements passed through a first-order filter, will exhibit a steady-state tracking error due to ramp-like (constant velocity) divergence and a continuously-growing tracking error in response to quadratic (constant acceleration) and higher order divergence inputs.

In a differential system such as LAAS, the airborne user and reference (LGF) tracking errors due to divergence will cancel precisely only if the ground and airborne filters are identical and sufficient time has elapsed since the initialization of each filter. In this work, we characterize and quantify the resulting differential error in the realistic case when these two conditions are not precisely satisfied. In this regard, ionospheric divergence has been modeled with ramp, quadratic, and harmonic (sinusoidal) structures. Using both time domain and frequency domain techniques, differential ranging errors due to ground-air differences in filter time constant, order, and initialization time are characterized.

This paper also includes analysis and experimental data that shows the magnitude of LAAS airborne error due to ionospheric spatial decorrelation. Since LAAS ground and aircraft receivers may be spatially separated by tens of kilometers, small variations in ionospheric delay between ground and air ionospheric pierce points result in small but non-negligible differential ranging errors at the aircraft. Furthermore, the effective separation between ground and aircraft is increased relative to their physical separation by an amount proportional to the filter time constant and the horizontal velocity of the aircraft. This paper derives the equation used to compute the standard deviation of this error at the aircraft and presents relevant experimental Wide Area Augmentation System (WAAS) data to estimate the standard deviation of the gradient of vertical ionospheric delay that is to be broadcast by the LAAS Ground Facility (LGF).

2.0 IONOSPHERIC DIVERGENCE

At the LAAS Ground Facility (LGF), a first order (Hatch) filter with 100 sec time constant is specified:

$$r(k) = \frac{N-1}{N}[r(k-1) + \phi(k) - \phi(k-1)] + \frac{1}{N}p(k)$$

where,

r is carrier-smoothed pseudorange
ϕ is carrier phase measurement output from receiver
p is pseudorange measurement output from receiver
τ_g is time constant of smoothing filter (100 sec)
ΔT is sample interval (1/2 sec)
N is $\tau_g / \Delta T$

The continuous analog to the Hatch Filter (taking limit as ΔT approaches zero) is [2]

$$\tau_g \dot{r}(t) + r(t) = \tau_g \dot{\phi}(t) + p(t) .$$

Taking the Laplace Transform yields

$$R(S) = \frac{\tau_g s \Phi(s) + P(s)}{\tau_g s + 1} .$$

We now consider the effect of a divergence error $e(t)$ such that

$$\phi(t) = e(t) \quad \text{and} \quad p(t) = -e(t) .$$

The resulting transfer function ffrom divergence input to the smoothed pseudorange output is

$$R(s) = \frac{\tau_g s - 1}{\tau_g s + 1} E(s) .$$

If a first order filter with a different time constant (τ_a) is used at the aircraft, the resulting differential ranging error is

$$\Delta R(s) = \frac{2(\tau_a - \tau_g)s}{\tau_a \tau_g s^2 + (\tau_a + \tau_g)s + 1} E(s) .$$

In the frequency domain, this is a band-pass filter with center frequency

$$\omega_{peak} = \frac{1}{\sqrt{\tau_a \tau_g}}$$

and peak gain

$$\left|H(j\omega_{peak})\right| = 2\frac{|\tau_a - \tau_g|}{\tau_a + \tau_g}.$$

Because of the band pass nature of the effective differential filter, it is clear that the differential ranging error due to high and low frequency divergence inputs will be suppressed. Figure 1 (left plot) shows an example time history of ionospheric delay collected over one hour period using dual frequency GPS carrier phase measurements. (The initial ionospheric delay, which has been arbitrarily set zero in the plot, is not relevant since it does not contribute to differential ranging error.) Also shown (right plot) is the Fourier Transform of the ionospheric delay overlaid on an example differential filter assuming a 100 sec time constant on the ground and a 150 sec time constant in the air.

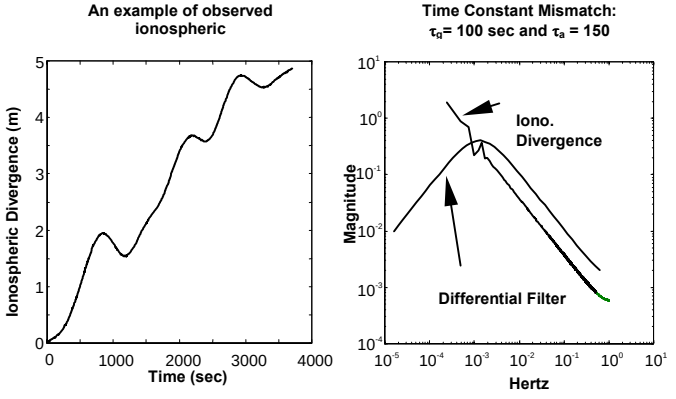

Figure 1. Divergence in the Frequency Domain

In the time domain, the steady state differential ranging error with respect to a *constant rate* divergence input $\dot{I}t$ is easily shown to be $2(\tau_a - \tau_g)\dot{I}$. For example, for an input rate of 1 cm/sec, ranging error will exceed 0.1 m if the two time constants differ by more than 5% (5 sec). Clearly, given the specified LGF time constant of 100 sec, only a small margin for aircraft design flexibility exists. The problem is made worse when higher order filters are used at the aircraft where, unlike the ground, ionospheric ramp inputs are tracked without steady state error. For these reasons, the LAAS Ground Based Augmentation System (GBAS) Standards and Recommended practices (SARPS) specifies that the ground and airborne filters must be identical. Because of the minimal design flexibility possible, this requirement does not represent a significant design constraint.

It is also important to note that these results also apply to carrier aided Delay-Lock Loops (DLLs) within ground and air receivers. However, the time constants are much smaller in this case. For example, at the LGF the minimum noise equivalent bandwidth of a carrier aided DLL is 0.125 Hz (which corresponds to a time constant of less than 2 sec). When the ground and air DLL time constants are individually small, their difference will also be small, resulting in negligible steady state differential ranging error.

Given that the ground and air filters have the same time constants, transient differential error due to divergence must still be considered. Transient error will always exist since, in general, ground and air filters will start tracking (and smoothing) a given satellite (SV) at different times. In the examples which follow, we assume that the reference receiver starts at time t = 0, while aircraft starts tracking at some later time $t = t_0$. (Note that the choice of which receiver starts tracking the SV first is arbitrary.)

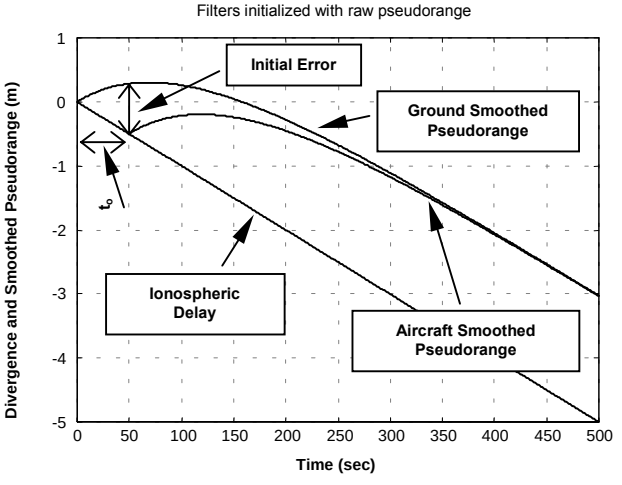

Figure 2. Example Response to Ionospheric Ramp

Figure 2 shows an example input ionospheric ramp of 1 cm/sec. Because the filters start at different times, differential error initially exists, but decays exponentially with time. Figure 3 shows parameterized curves of transient differential ranging error for a number of air filter start times (t_0). In this figure the parameter a_1 represents the ionospheric ramp slope $\dot{I}$. The worst-case differential error occurs when the ground filter is at (or near) steady state when the aircraft filter begins tracking the satellite.

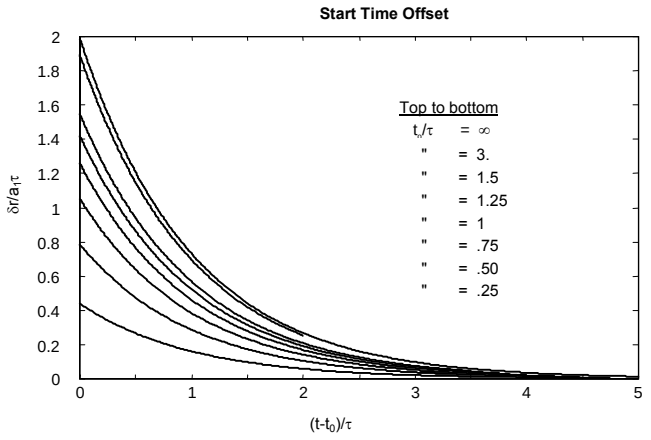

Figure 3. Normalized Transient Ranging Error (Ramp Input)

In Figure 3 the curve labeled ($t_0/t = \infty$) corresponds to this case. In this scenario, for a 1 cm/sec input ionospheric ramp, transient differential error will be larger that 10 cm unless a 300 sec wait time has elapsed before the aircraft smoothing filter output is used.

It is worth noting that if divergence rate is *known*, the filters can be started at steady state. In this case, there will be no transient response to ramp inputs. Unfortunately, estimation of divergence rate from the single frequency (code-minus-carrier) data available to LAAS will also require smoothing over time to mitigate effect of multipath. In this context, the wait-time is not avoided, but instead simply passed over to another process.

It is also desirable to consider the effect of higher order inputs. In this regard, it is natural to next consider to the case of a quadratic input. However, the first order filters to be implemented in LAAS will not track quadratic (or higher order inputs) with a steady state error; the error will instead continue to grow with time.

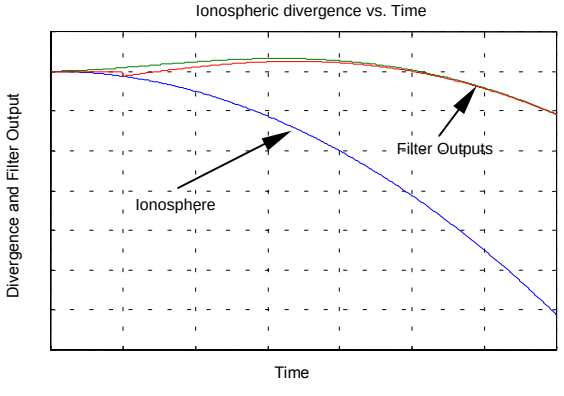

Figure 4. Example Response to Ionospheric Quadratic Input

Figures 4 and 5 show the results for quadratic inputs (with $a_2 =) \ddot{I}$ analogous to those of Figures 2 and 3 for ramp inputs. In this case, no worst-case value of t_0 exists (and only results up to $t_0/\tau = 7$ are shown in Figure 5). Therefore, no specific wait time is sufficient. However, it is important to note that quadratic inputs due to the ionosphere cannot be sustained indefinitely. A more realistic model is needed to characterize the effects of higher order inputs.

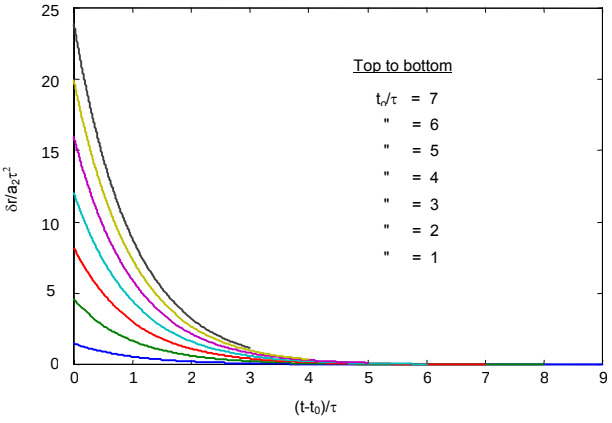

Figure 5. Normalized Transient Ranging Error (Quadratic Input)

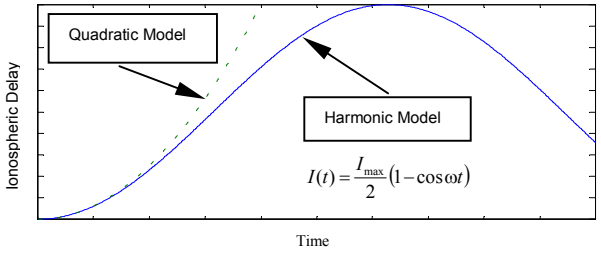

Figure 6. Inonospheric Harmonic Input

As illustrated in Figure 6, a harmonic model (sine/cosine input) implicitly includes quadratic and higher order effects while simultaneously maintaining the bounded maximum amplitude of ionospheric delay. In this case, the transient differential error depends on two factors: the phase shift (time offset) between initialization of the two filters and the input ionospheric frequency. In Figure 7, an example ionospheric input with 500-second period is shown together with resulting the ground filter response and several potential air filter responses corresponding to different initialization times. It is clear that over time the ground and air filter outputs will converge and the resulting differential ranging error will approach zero. In the transient region, however, differential ranging error will exist.

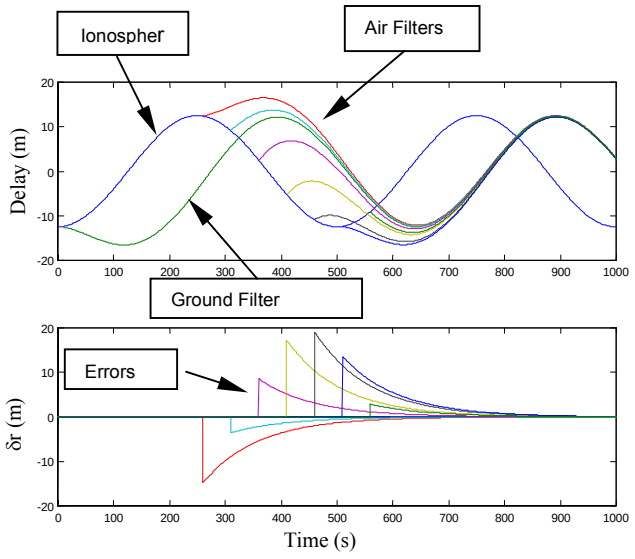

Figure 7. Example Resonse to Harmonic Input

The phase (time) offset between the ground and airborne filter initialization that leads to maximum transient differential error will depend on the input frequency. It is also important to consider the fact that the amplitude of the ionospheric input (I_{max}) should become smaller as frequency (ω) increases. In this analysis, we assume a maximum ionospheric delay amplitude of 30 m applicable to the diurnal frequency (~10^{-5} Hz). Amplitudes of ionospheric inputs at higher frequencies are modeled as proportional to $1/\omega$. This model is reasonably consistent collected data.

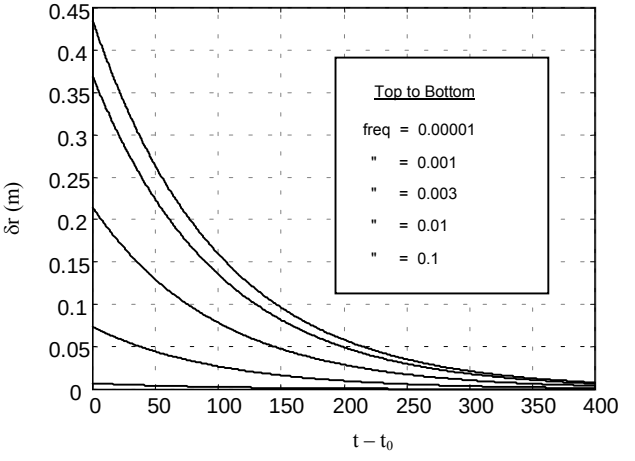

Figure 8. Worst-Case Transient Response to Harmonic Input

Figure 8 shows the worst-case transient differential ranging error for several input frequencies. In these results it seen that errors less that 10 cm are achievable with a maximum wait time of approximately 150 sec. By comparison, the results for the ramp input case are more conservative.

While the results from the models considered are clearly sensitive to the specific quantitative assumptions made regarding ramp input magnitude and amplitude vs. frequency characteristic, the methodologies are useful for determining acceptable wait times for first use of LAAS filter outputs. It is also important to note that the wait time can be circumvented by appropriate inflation of the measurement error standard deviations used to compute vertical and horizontal protection levels for LAAS. In this case, an exponentially decaying error component may be included in the overall LAAS error model to compensate for the transient differential error resulting from ionospheric divergence.

3.0 IONOSPHERE SPATIAL DECORRELATION

In addition to residual differential ionosphere errors from divergence (temporal decorrelation), LAAS users will also encounter small errors due to spatial decorrelation, or the change in ionspheric delay between user and reference receiver ionospheric "pierce points." In order to insure that computed user protection levels bound actual errors throughout the LAAS coverage volume, the LAAS VHF data broadcast includes a standard deviation of ionosphere spatial variation, $\sigma_{vert\_iono\_gradient}$ (or σ_{vig}), in the Type 2 message. This parameter has an 8-bit message field with a least-significant-bit resolution of 0.1 mm/km, allowing a maximum value of 25.5 mm/km to be transmitted.

User Error due to Ionospheric Spatial Gradient

The following equation relates vertical ionospheric spatial decorrelation (dI_v/dx) to pseudorange error for a given GPS satellite:

$$\Delta I_v(t,x) = \hat{I}_{v,a} - \hat{I}_{v,g} \approx \frac{dI_v}{dx}[x_a + 2\tau_a v_a]$$

where τ_a is the airborne smoothing time , v_a is the aircraft lateral velocity, and x_a is the LGF-to-aircraft separation. This equation gives the vertical ionosphere change, which must be multiplied by an obliquity factor (F_{PP}) to convert to actual (slant) range error [3]:

$$F_{pp} = \left[1 - \left(\frac{R_e \cos(\theta)}{R_e + h_I}\right)^2\right]^{-\frac{1}{2}}$$

where R_e is the approximate radius of Earth (6378.136 km), and h_I is the approximate ionosphere shell height (taken to be 350 km). Note that this factor varies from 1.0 for satellites directly overhead to greater than 3.0 for low-elevation satellites. These equations are used in the following figures to relate σ_{vig} to σ_{iono}, which is the one-sigma differential user range error. These plots assume τ_a = 100 sec (to match the LGF) and a constant τ_a = 70 m/sec for a jet aircraft during approach.

Figure 9 shows the resulting vertical ionosphere error for three different values of σ_{vig} as a function of LGF-user separation. For σ_{vig} = 2 mm/km, the one-sigma error at a conservative approach-threshold distance from the LGF (x_a = 7.5 km) is 4.3 cm, which is negligible compared to multipath and other LGF error sources. At the edge of LGF VDB coverage (x_a = 23 n.mi., or about 43 km), the error is about 11.8 cm, which is still small and is much less significant because the required protection levels at this distance from the LGF are much larger than those that apply at the approach threshold. Figure 10 shows the impact of σ_{vig} = 4 mm/km and σ_{vig} = 25.5 mm/km (the maximum possible broadcast value) on the total user range error for Ground Accuracy Designator B3 and Airborne Accuracy Designator A. For σ_{vig} = 4 mm/km, the increase in user range error sigma due to ionospheric effects is no greater than 12.5%; thus the impact on user availability is very small. On the other hand, σ_{vig} = 25.5 mm/km increases overall user error sigma by a factor of 3 or more, which would dramatically impact user availability. While it is not possible to determine the maximum possible ionosphere spatial gradient that might ever occur, it makes little sense to field a LAAS system with σ_{vig} = 25.5 mm/km without using some other means of ionosphere estimation (dual-frequency measurements, WAAS) to reduce the error. Thus, a maximum message field value of 25.5 mm/km for σ_{vig} is sufficient.

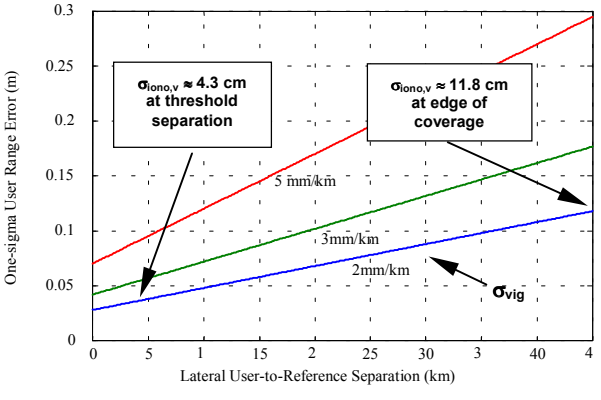

Figure 9. User Differential Ionosphere Errors

Because LAAS uses single-frequency (L1-only) reference receivers and does not observe ionosphere delays in real time, it must broadcast values of σ_{vig} that overbound the true ionosphere gradients under worst-case conditions. In order to examine the values of σ_{vig} that may occur under worst-case conditions, we have used the Raytheon WAAS database of ionosphere "supertruth" data of delays at the pierce points of the 25 WAAS reference stations [5]. This data has limited applicability to LAAS because most WAAS pierce-point separations are well over 100 km, whereas LAAS users are most interested in separations well below 100 km. However, sufficient data exists for separations of 400 km and less to allow us to "zoom in" and make reasonable inferences regarding very-short-range ionosphere delay differences.

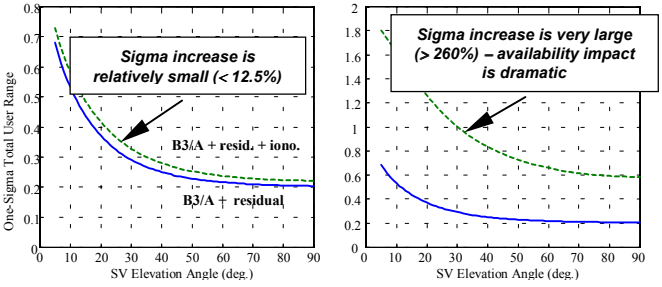

Figure 10. Contribution of Ionosphere Errors to Total User Error (B3/A Case)

Figure 11 shows the cumulative distribution function (cdf) of ionosphere delay differences between pierce points for CONUS reference stations on April 7, 2000, when a major ionosphere storm took place. Each line in the plot represents a specific pierce-point separation (the data were binned according to separation between 0 and 400 km so that separate histograms could be plotted). These distributions appear roughly Gaussian but with slightly fatter-than-Gaussian tails. This does not necessarily mean that the underlying data is non-Gaussian. Instead, it may be an artifact of "mixing" data from many different reference stations with slightly different ionosphere delay distributions [4].

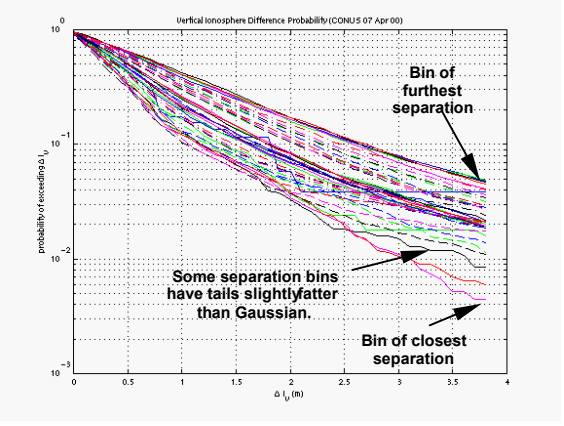

Figure 11. CDF of CONUS Ionosphere Gradients, 7 April 2000

Figure 12 shows the values of σ_{vig} estimated from the 68th and 95th percentiles of these cumulative distributions as a function of pierce-point separation. Note that these values are non-zero even for zero separation because of errors in the obliquity conversion between vertical and slant errors for satellites tracked by different reference stations and residual L1/L2 interfrequency biases. These errors do not affect LAAS users because L2 is not used to correct for ionospheric delays and because obliquity differences between LAAS reference and user receivers tracking a given satellite will be very small. Therefore, it is the slope of these lines that is of interest to LAAS. In this plot, the same slope is obtained for both percentiles and is consistent over pierce-point separations between 75 and 375 km: $\sigma_{vig} \cong 2.7$ mm/km.

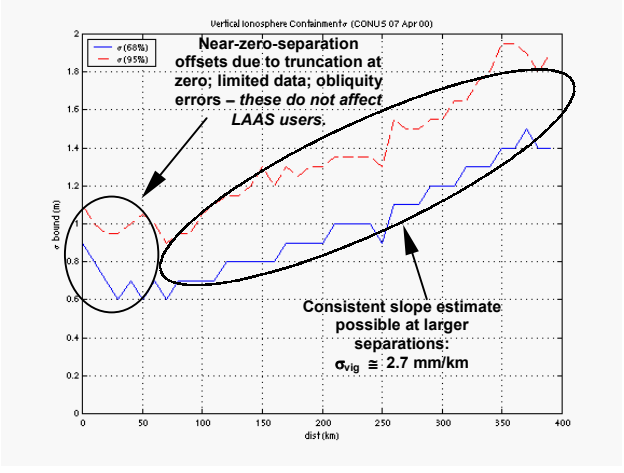

Figure 12. σ_{vig} for CONUS Ionosphere, 7 April 2000

Figures 13 and 14 show the same results as Figures 11 and 12 for April 6, 2000, the day of onset of the ionospheric storm. Figure 13 shows very obvious tail fattening due to mixing sets of data with very different variances: the pre-storm ionosphere delays and those occurring after storm onset. Figure 14 shows that this mix of two sets of data causes the sigma estimated from the 68th percentile to be lower than that of the 95th percentile. However, both April 6 sigma estimates (1.3 and 1.9 mm/km) are lower than the estimate for April 7.

It should be noted that the gradients observed on these two storm days are much larger than typical gradients observed in CONUS on non-storm days, even during solar maximum, when σ_{vig} for CONUS is no greater than 1.0 mm/km and is typically 0.5 mm/km or less. However, as noted above, LAAS has no direct means of observing which days are nominal and which have ionosphere storms; thus the broadcast σ_{vig} must reflect possible storm events in order to be an overbound at all times. The data examined to date suggests that in CONUS, a broadcast σ_{vig} of 4 mm/km will be a sufficiently conservative overbound. However, more recent storm data collected in CONUS on July 15-16, 2000 must be investigated to confirm that this value overbounds that event as well [5].

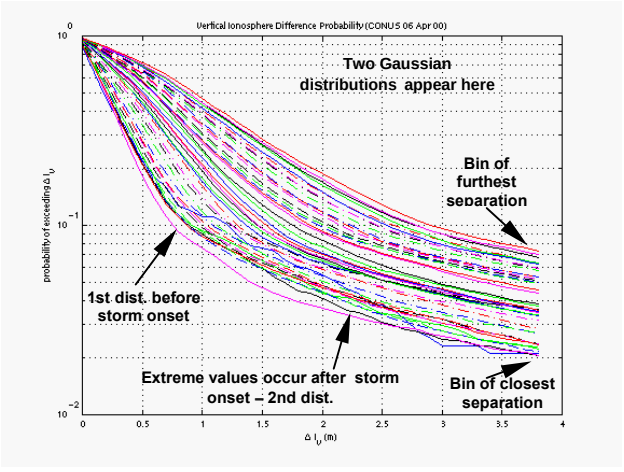

Figure 13. CDF of CONUS Ionosphere Gradients, 6 April 2000

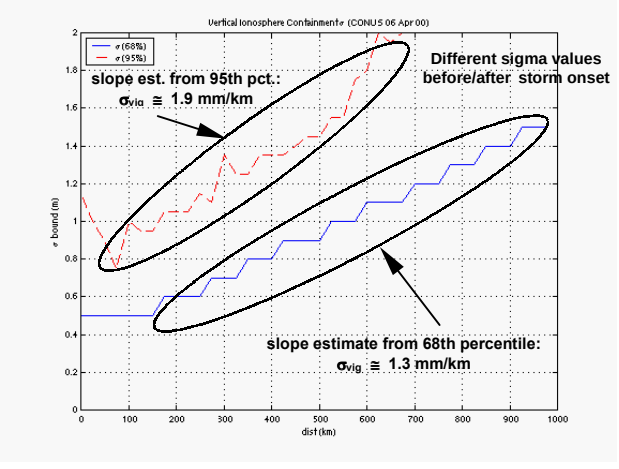

Figure 14. σ_{vig} for CONUS Ionosphere, 6 April 2000

Figures 15 – 18 show plots of ionosphere gradient cdf's and resulting sigma estimates for data taken by the single WRS in Hawaii on the same two days as shown previously for CONUS. There are far fewer points in this data; thus the maximum separation bin has been increased to 800 km, and the results appear "noisier." The CDF plot in Figure 15 for April 7 shows that the ionosphere gradients are larger in Hawaii than in CONUS, which is expected because Hawaii is on the northern edge of the equatorial region of the ionosphere, where delays and gradients are significantly larger. Note that the tails in Figure 15 appear narrower than Gaussian, which may be because the data is taken from only one site and no

"mixing" is occurring. The sigma estimates for April 7 in Figure 16 are consistent and give $\sigma_{vig} \cong 4.1$ mm/km.

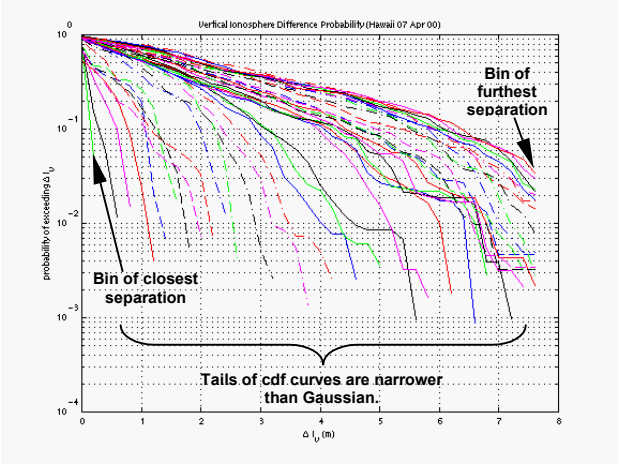

Figure 15. CDF of Hawaii Ionosphere Gradients, 7 April 2000

Figures 17 and 18 are for Hawaii on April 6. The cdf plot in Figure 17 is similar to that of Figure 15 but shows slightly fatter tails, which may be due to the impact of mixing pre-storm and storm data. Figure 18 shows that some tail fattening is present in the data, as significantly different σ_{vig} values (3.7 and 5.5 mm/km) are estimated from the 68th and 95th percentiles of the data, respectively. The larger of these values significantly exceeds the 4.1 mm/km observed on April 7.

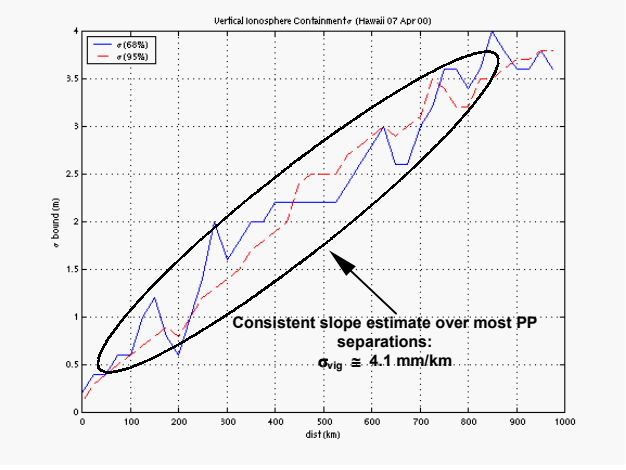

Figure 16. σ_{vig} for Hawaii Ionosphere, 7 April 2000

Based on this limited set of data, it is very difficult to select a value of σ_{vig} that we can confidently state to be an overbound for LAAS stations in Hawaii. A value of roughly 8 mm/km would give some margin over the worst results observed from this data, but more data needs to be taken, and the July 15-16 storm data should be investigated as well. Even if 8 mm/km were sufficient for Hawaii, it is not at all clear that it would suffice for LAAS sites deeper in the equatorial region. For example, recent data from Brazil suggests that the worst-case ionosphere spatial gradients observed there may be significantly larger than 8 mm/km [6]. If this is the case, broadcasting larger values of σ_{vig} would significantly impact the user error budget and thereby reduce availability. It would be better use of real-time dual-frequency data obtained locally or via SBAS to reduce the size of these gradients.

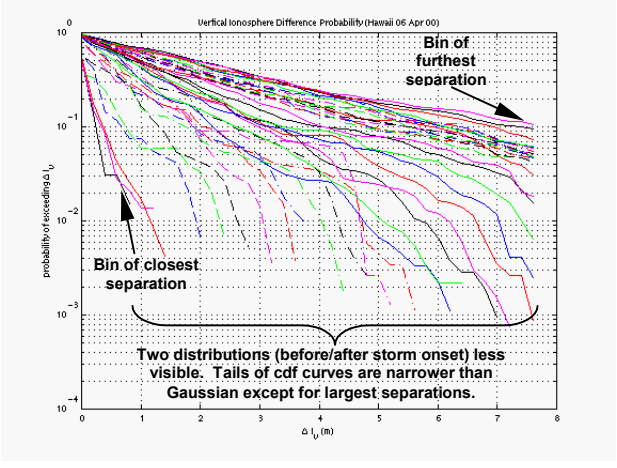

Figure 17. CDF of Hawaii Ionosphere Gradients, 6 April 2000

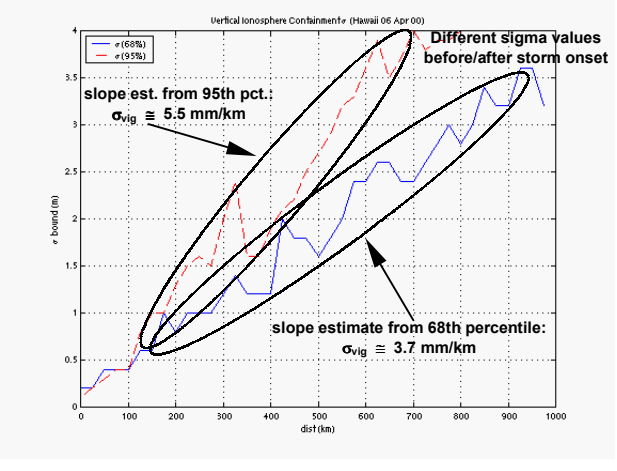

Figure 18. σ_{vig} for Hawaii Ionosphere, 6 April 2000

4.0 SUMMARY AND FUTURE WORK

It has been shown that for safe interoperability of single frequency ground/air smoothing filter implementations in the presence of ionospheric divergence, only very small

(5-10 sec) differences in time constant are permissible. Because of this relatively minimal design flexibility, the existing GBAS requirement that smoothing filter time constants be matched at 100 sec is not a significant additional design restriction. Carrier-aided DLL implementations are interoperable because minimum noise-equivalent bandwidth is typically large. A minimum bandwidth of 0.125 Hz is required by LGF specification; airborne implementations should use a similarly large value.

To ensure the transient differential error due to divergence is small, both ground and air filters should be near steady state. The results of constant rate and harmonic divergence input models suggest that wait times less than 300 sec are likely sufficient to keep ranging error below 10 cm. An alternative technique to accommodate transient differential error without waiting is to inflate the error standard deviation of the smoothed pseudorange. The inflation factor implemented for this purpose would decay exponentially with time as the filters approach steady state.

Ionospheric spatial decorrelation induces small errors for LAAS users. LAAS ground facilities will broadcast conservative standard deviations (that reflect worst-case ionospheric-storm conditions) of ionosphere spatial gradients at each LAAS site, and LAAS users will apply a simple equation to convert these gradients to sigmas of user range error due to spatial decorrelation based on their separations from the LAAS ground facility and their appoach velocities. "Supertruth" data showing ionosphere delay differences between WAAS reference station has been studied to estimate the standard deviations of ionosphere spatial gradients under recent ionosphere storm conditions. While one-sigma gradients under nominal conditions are typically no greater than 0.5 mm/km, a sigma of 2.7 mm/km was observed in CONUS during the April 7 storm, and a sigma of 5.5 mm/km was estimated from a smaller set of Hawaii data on the storm onset day of April 6.

More work is needed to make more confident assessments of the spatial decorrelation sigmas that should be broadcast in CONUS and in equatorial regions. Data from the July 15-16, 2000 storm will be examined to see if the spatial decorrelations during that storm exceed those found during the April 6-7 storm or the projected CONUS broadcast value of 4 mm/km. For Hawaii and other equatorial regions, data from more reference sites is needed to make better estimates of the spatial-gradient sigmas that occur during worst-case conditions. Another issue of interest is the structure of ionospheric correlation across different satellites visible to a single LAAS ground facility. The current method of computing range error sigmas for individual satellites assumes that the errors are uncorrelated. This may be conservative in the case of ionospheric spatial gradients because the same stucture of ionosphere delay variation affects all satellites in view of a single location. The component of ionosphere spatial variation that is common to all satellites in the user's position solution will not affect his or her position error because it will be absorbed by the user clock solution. Accordingly, it may be possible to take credit for this correlation to reduce the values of σ_{vig} that are transmitted by LAAS ground facilities.

ACKNOWLEDGEMENTS

The help of Todd Walter, Andrew Hansen, and the Raytheon WAAS team that supplied us with WAAS "supertruth" data is greatly appreciated, as is funding support from FAA AND-700. The opinions discussed here are those of the authors and do not necessarily represent those of the FAA or other affiliated agencies.

REFERENCES

[1] P. Hwang, G. McGraw, and J.Bader, “Enhanced Differential GPS Carrier-Smoothed Code Processing Unit Dual-Frequency Measurements,” *J. of the Institute of Navigation*, Vol.46, No.2 (1999),pp. 127-137.

[2] B. Pervan, “Code-Carrier Divergence Analysis for LAAS,” Briefing to RTCA SC-159 WG-4, Washington, D.C., November 3, 1998.

[3] *Minimum Operation Performance Standards for Global Positioning System/Wide Area Augmentation System Airborne Equipment*. Washington, D.C., RTCA, DO-229B, Oct. 6, 1999.

[4] J. Parker, "The Exponential Integral Frequency Distribution," *J. of the Institute of Navigation* (London), Vol. 19, No. 4 (1966), pp. 526-529.

[5] A. Hansen, *et.al.*, "Ionospheric Spatial and Temporal Correlation Analysis for WAAS: Quiet and Stormy," *Proceedings of ION GPS 2000*. Salt Lake City, UT., Sept. 19-22, 2000.

[6] S. Skone, "Wide Area Ionosphere Modeling at Low Latitudes: Specifications and Limitations," *Proceedings of ION GPS 2000*. Salt Lake City, UT., Sept. 19-22, 2000.